Control of Linear Motors for Machine Tool Feed Drives: Experimental Investigation of Optimal Feedforward Tracking Control[1]

David M. Alter[2,3] and Tsu-Chin Tsao[2]

This paper investigates the use of optimal l_1 and H_∞ model reference optimal feedforward control to enhance the tracking performance of a linear motor drive. Experimental work is presented which studies the effects of signal preview, tracking constraint, and reference model choice on tracking performance. Suboptimal l_1 control where the closed-loop system has a zero on the unit circle due to integral action in the feedback controller is given special attention, and is seen to give near optimal performance for the system under study here. For the specific trajectory employed here, the best performing feedforward controllers were experimentally seen to reduce by more than half the maximum and rms tracking errors of the H_∞ optimal feedback closed-loop systems.

1 Introduction

Direct electric feed drives have come under study relatively recently for use in next generation high-speed machine tools. To exploit the high-speed and acceleration of direct linear drives for machine tool applications, the drive control must achieve as high as possible tracking performance and dynamic stiffness. By augmenting the H_∞ optimal position feedback loop for maximum dynamic stiffness (Alter and Tsao, 1996), this paper presents an experimental investigation of the l_1 and H_∞ optimal feedforward tracking control from (Tsao, 1994) to improve the tracking performance, with the two optimal norm cases being presented in parallel. Special attention is given to a practically important case where the feedback controller has integral action. In this case, an optimal solution to the l_1 problem does not generally exist due to the existence of a unit circle zero in the model matching formulation.

The l_1 norm of a transfer function impulse response is the induced norm of l_∞ (i.e., bounded) signals. Hence, minimizing the l_1 norm of the tracking error system minimizes the maximum error value over all bounded reference trajectories. Alternately, the H_∞ norm of a transfer function is the induced norm of l_2 (i.e., finite energy) signals, and is also equal to the input-output ratio of rms signal power. Thus, minimizing the H_∞ norm of a tracking error system minimizes the worst case rms error ratio. The l_1 norm seems particularly applicable to machine tool applications since it provides a direct and useful measure of the part geometric tolerance.

Some notation used in this paper will now be clarified. Consider the discrete linear time-invariant system whose impulse response is denoted as $h(k)$, $k = 0, 1, 2, \ldots, \infty$. Its induced l_1 system norm may be computed as

$$|h(k)|_1 = \sum_{k=0}^{\infty} |h(k)|.$$

Also, the Z-transform of $h(k)$ is denoted as $H(z)$:

$$H(z) := \sum_{k=0}^{\infty} h(k) z^{-k}.$$

For optimal design purposes, it is most convenient to define system transfer functions in the λ domain, where λ is related to the conventional Z-transform variable z by $\lambda = z^{-1}$. Denoting the set of proper stable rational functions by $\mathcal{R}_\infty$, it is clear that a system in the λ domain is BIBO stable if and only if its transfer function has all of its poles *outside* the unit circle in the complex plane.

2 Optimal Feedforward Problem Formulation

Figure 1 depicts the block diagram of feedforward controller implementation, where P_1 is the plant, C_{ff} and C_{fb} are the feedforward and feedback controllers, and M_0 is a reference model with a desired tracking property. The model following error $e(k)$ is

$$e(k) = [M' - GC_{ff}]r(k) \tag{1}$$

where

$$M' = M_o - (P_1C_{fb})/(1 - P_1C_{fb})$$
$$\text{and} \quad G = P_1/(1 + P_1C_{fb}) \tag{2}$$

Note that M' and G are known after the design of C_{fb}.

It will be seen in the next section that the solution methods to H_∞ and l_1 optimal feedforward problems depend upon the unstable zeros of G. The zeros of G contain the unstable plant zeros (i.e., zeros of P_1) and unstable feedback controller poles. Although other feedforward control configurations exist, an advantage of this one is that the tracking error signal (e) is preserved in the block diagram, and the proportion of the control input signal attributable to the feedforward and feedback controllers can be readily determined. Also, the unity d.c. gain, if the feedback controller is designed with integral action, is preserved for any feedforward controller.

Since C_{ff} is required stable for obvious reasons, the optimal tracking performance, based upon the induced norm of the error system, may be defined in linear affine form over the stable free parameter C_{ff}:

$$J_{(\cdot)}^{opt} = \inf_{C_{ff} \in \mathcal{R}_\infty} \|M' - GC_{ff}\|_{(\cdot)} \tag{3}$$

where $(\cdot)$ represents in this case the l_1 or H_∞ norm. If the infimum is achieved by some C_{ff}, it is called the optimal tracking controller.

Because the l_1 or H_∞ induced norm used in (3) is minimized over a large class of reference input signals, namely norm bounded signals, the resulting feedforward tracking controller is usually overly conservative and does not give good tracking performance, as will be seen from the experimental results presented in a later section. To achieve better tracking performance for practical input reference signals such as those with speed

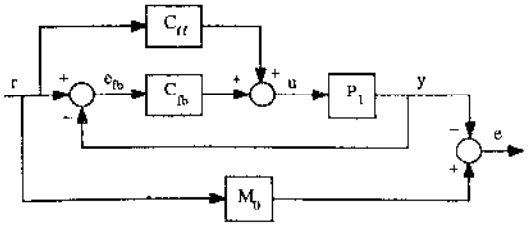

Fig. 1 Block diagram for feedforward formulation

[1] This work was supported in part by National Science Foundation, Grant No. DDM-90-09830

[2] Department of Mechanical and Industrial Engineering, University of Illinois at Urbana-Champaign, Urbana, IL 61801.

[3] Presently with Texas Instruments, Inc., Dallas, Texas.

Contributed by the Dynamic Systems and Control Division of THE AMERICAN SOCIETY OF MECHANICAL ENGINEERS. Manuscript received by the Dynamic Systems and Control Division June 1994. Associate Technical Editor: O. Nwokah.

or acceleration limit, Tsao (1994) presented means to limit the reference signals to smaller classes. The remainder of this section briefly reviews the methods formulated therein. Notation will be given for the l_1 optimal problem. The H_∞ optimal problem can be obtained by simply replacing in the applicable places the signal norm l_∞ with l_2, and the transfer function norm l_1 with H_∞.

Reference Trajectory Preview. This gives the controller the ability to anticipate trajectory behavior, and to compensate for the dynamic delay of the plant. The optimal feedforward tracking problem is solved by simply using $r(k + N_p)$ as the trajectory input to the system and by replacing M_0 with $\lambda_p^N M_0$.

Reference Trajectory Constraint. The reference signal is assumed generated by filtering an unknown signal v through an unstable transfer function T^{-1}:

$$r = T^{-1}v \quad \text{where} \quad T \in \mathcal{R}_\infty$$

$$\text{but} \quad T^{-1} \notin \mathcal{R}_\infty, \quad \text{and} \quad v \in L_\infty. \quad (4)$$

When formulating the constrained optimization problem, the error system is defined as $E := M' - GC_{ff}$, and one seeks C_{ff} so that $E = E'T$ for some $E' \in \mathcal{R}_\infty$. Minimizing the induced norm of the constrained error system E' leads to the following result:

$$\sup_{\|Tr\|_\infty \le 1} \|Er\|_\infty = \sup_{\|Tr\|_\infty \le 1} \|E'Tr\|_\infty = \sup_{\|v\|_\infty \le 1} \|E'v\|_\infty = \|E'\|_1. \quad (5)$$

In this way, it is possible to minimize the model following error for a class of reference trajectories with limited velocity or limited acceleration by choosing $T = (1 - \lambda)$ or $T = (1 - \lambda)^2$, respectively. Such *speed limits* are of interest in machining since they may be adjusted at the path planning stage of the machining process. Referring to (5), one sees that if the velocity or acceleration bound is $\|v\|_\infty = \alpha$, then the maximum model following error is $\alpha\|E'\|_1$. This result may be used to perform mechanical tolerance control if desired.

The constraint $E = M' - GC_{ff} = TE'$ is incorporated into the framework for optimal feedforward tracking by rearranging it into the Diophantine equation $GC_{ff} + TE' = M'$. Provided that G and T are coprime, all solutions to the Diophantine equation are

$$[C_{ff}, E'] = [XM' + TQ, YM' - GQ], \quad Q \in \mathcal{R}_\infty \quad (6)$$

where $X, Y \in \mathcal{R}_\infty$ are solutions to the Bezout identity $GX + TY = 1$. Therefore, the constrained optimal tracking problem may be written as

$$J_{(\cdot)}^{\text{opt}} = \inf_{Q \in \mathcal{R}_\infty} \|M - GQ\|_{(\cdot)} \quad (7)$$

where $M = YM'$, and C_{ff} is obtained from (6) after solving (7). Note that the chosen preview length and reference model are embedded in M' and that the actual tracking error differs from the model following error unless $M_0 = 1$. A weighting filter W could also be placed in (7) for frequency weighted optimization but it is not used here because the reference model M_0 has a similar effect.

3 Optimal Feedforward Problem Solutions

Solution techniques for linear affine optimization problems of the form (7) are well established for the H_∞ and l_1 norms. In general, these methods do not allow G to contain any unit circle zeros One technique for obtaining the *no unit circle zero* solution in the H_∞ case may be found in (Zames and Francis, 1983). A general solution for the no unit circle zero l_1 problem may be found in (Dahleh and Pearson, 1987). It can be shown that if G has only one unstable (non-unit circle) root, the solutions to the l_1 and H_∞ minimization problems are identical, i.e., $Q_1^{\text{opt}} = Q_\infty^{\text{opt}}$ and $J_1^{\text{opt}} = J_\infty^{\text{opt}}$ (Vidyasagar, 1991). Note that any number of origin zeros common to both $G(\lambda)$ and $M(\lambda)$ may be factored out of either minimization problem. If only one nonorigin unstable zero of G remains, the l_1 and H_∞ solutions are identical in this case too.

The linear motor continuous-time domain transfer function is of relative order 3. The zero-order hold λ domain transfer function of a relative order 3 system always has one unstable zero at the origin, and another unstable zero approaching -0.2679 as the sampling period approaches zero. Depending upon the position feedback controller used in the servo-loop, the previous paragraph suggests that it is possible to design a feedforward controller which simultaneously gives optimal tracking in both the l_1 and H_∞ sense. This implication is applicable to many electro-mechanical servo systems, which may be modeled similar to the linear motor.

The above solution methods are not directly applicable when G contains unit circle zeros, which is a case that is of some practical interest. For example, servo-loops which asymptotically reject step disturbances (i.e., integral action) will contain a zero at $\lambda = 1$ due to the pure integrator in the controller. Special treatment of this case, where G contains a zero at $\lambda = 1$ will be based upon the following observation: if the reference model M_0 has unity D.C. gain, then M' as defined in (2) will contain the same unit circle zero at $\lambda = 1$ that G does. This is a subcase of the more general situation where all unit circle zeros of G are common to M (termed the *common unit circle zero case*).

The optimal H_∞ solution in the common unit circle zero case may be found by solving a sequence of problems where the unit circle zeros are perturbed to the stable region, with the perturbations converging to zero (Vidyasagar, 1985). The optimal l_1 problem is more difficult however, and, in fact, no general solution method is currently documented. The l_1 problem was investigated in (Vidyasagar, 1991), a work that produced several results of interest here. First, a method was given for computing the optimal cost J_1^{opt}. Second, it was shown for the common unit circle zero case that the perturbation method used for the H_∞ problem does not in general converge to the optimal solution in the l_1 case. However, a convenient method for computing the sub-optimal cost of the converged controller was presented. A measure of suboptimality is thus available, from which it might turn out that the sub-optimal controller obtained via the perturbation technique will provide sufficient performance.

Referring to the definition of G given in (2), and assuming an integral action (but otherwise stable) feedback controller C_{fb}, it is seen that G will contain an unstable origin zero, a single unit circle zero at $\lambda = 1$, and (provided that the sampling rate is sufficiently fast) a single negative unstable zero. It will be assumed that the reference model and preview length combination have been selected so that $\lambda_p^N M_0 = 0$ at $\lambda = 0$, and that the resulting single zero at the origin common to both G and M' has been factored out of the norm. The following corollary, produced by applying the results of Vidyasagar's work, characterizes the l_1 optimal cost and the sub-optimality of the perturbation method solution:

Corollary 1. Consider the following optimization problem:

$$J_1^{\text{opt}} = \inf_{Q \in \mathcal{R}_\infty} \|M - GQ\|_1, \quad M, G, Q \in \mathcal{R}_\infty$$

where $M(1) = 0$, and $G(\lambda) = [(\lambda - 1)(\lambda - b)/(1 - b\lambda)]G_o$ with $b < 0$, $|b| < 1$, and $G_o^{-1} \in \mathcal{R}_\infty$.

$$\text{Define} \quad G_\epsilon := \frac{(\lambda - b)}{(1 - b\lambda)} G_o$$

$$\text{and construct} \quad Q_\epsilon = \frac{Q_0}{(\lambda - 1 - \epsilon)}$$

where $\epsilon > 0$ and Q_0 denotes the unique optimizing solution to the problem with G_ϵ in place of G. Finally, let $J_1^\epsilon := \|M - GQ_\epsilon\|_1$. Then

$$J_1^{\epsilon,\text{opt}} = \frac{2}{1-b}\,|M(b)| \quad \text{and} \quad \lim_{\epsilon \to 0} J_1^\epsilon = 2|M(b)|.$$

Proof: See Appendix.

The degree to which Q_ϵ is suboptimal is thus determined solely by the location of the single unstable zero of G. On one extreme we have $b = -1$ which produces a worst case suboptimality factor of two. On the other hand, it is seen as $b \to 0^-$ that Q_ϵ does indeed converge to the optimal solution. This last observation represents a borderline case of a result pointed out by Vidyasagar, where he states that Q_ϵ converges to the optimal solution if the single unstable zero of G is positive.

4 Experimental Results

The hardware used here is the same AURA HFA-100/6 linear motor utilized in Alter and Tsao (1996) and the reader is there referred for hardware and modeling information. The two H_∞ optimal feedback controllers, controller design A and B presented therein, are used in this paper and referred as the same. Controller A does not have integral action while controller B has integral action, resulting in a unit circle zero for feedforward controller design. At the same sample rate of 2000 Hz, the λ-domain zero-order hold equivalent of the model $P_1(s)$ contains an unstable origin zero, and another unstable zero at $\lambda = -0.3075$. The reference model M_0 and constraint T have been chosen as

$$M_0 = 0.25(\lambda^{-1} + 2 + \lambda)^m \quad T = (1-\lambda)^N$$

along with a preview length $N_p \geq m$. M_0 is a zero-phase low-pass filter of order m, while T represents the fact that the N^{th} difference of the reference trajectory is bounded by some known value. Note that the noncausal M_0 requires a minimum preview length of $N_p = m$.

The reference trajectory chosen for tracking performance evaluation is composed of step, ramp, and parabolic elements, and is representative of a type commonly used in machine tool drives. The wave form and its first difference are plotted in Fig. 2. The trajectory was actually implemented as a repetitive signal, such that this plot represents a single cycle from a periodic wave form. Subsequent result plots have their time step axes aligned with that in this figure. The trajectory has a maximum values of displacement at 0.0266 m, speed at 0.38 m/s, acceleration at 7.6 m/s^2 and jerk at 15200 m/s^3, respectively.

At this point, tracking results using optimal feedforward control designed from Eq. (7) in combination with feedback controller A are presented in Table 1 and will be discussed in the next few subsections. The theoretical tracking results shown in the table were generated by simulation using the discrete time model. Note that all *tracking error* results presented in the remainder of this paper represent actual tracking errors, as opposed to model following errors. Note also that the feedforward controllers for l_1 and H_∞ optimality in Table 1 are actually the same, as discussed in the previous section. It is only the interpretation of the tracking data that differs. Experimental results are generally shown to the nearest micron (the position sensor resolution is $\pm$ 2 μm), although a minimum of 2 significant figures is always given. A minimum of 3 significant figures is given for theoretical results. As a baseline for performance comparison, the feedback controllers A and B were first evaluated without feedforward control (line 29 Table 1, and line 33 Table 3).

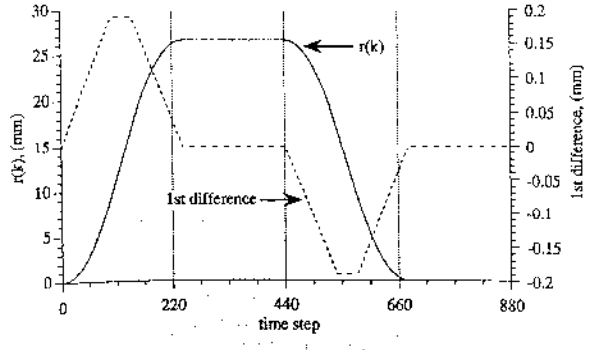

Fig. 2 Reference trajectory

Table 1 Tracking results using optimal feedforward control designed for feedback controller A

	Design Parameters			max. tracking error (m)		tracking error rms (m)	
#	m	N_p	N	exper.	theor.	exper.	theor.
1	0	0	0	2.6600e-2	2.6600e-2	1.7552e-2	1.7552e-2
2	0	1	0	2.6600e-2	2.6600e-2	1.7552e-2	1.7552e-2
3	0	2	0	8.178e-3	8.178e-3	5.396e-3	5.396e-3
4	0	3	0	2.524e-3	2.515e-3	1.659e-3	1.959e-3
5	0	4	0	7.77e-4	7.73e-4	5.08e-4	5.10e-4
6	0	5	0	2.48e-4	2.38e-4	1.57e-4	1.57e-4
7	0	6	0	8.1e-5	7.31e-5	4.9e-5	4.82e-5
8	0	7	0	3.2e-5	2.25e-5	1.6e-5	1.48e-5
9	0	8	0	2.5e-5	6.91e-6	8.1e-6	4.56e-6
10	0	9	0	1.9e-5	2.12e-6	6.9e-6	1.40e-6
11	0	10	0	1.9e-5	6.53e-7	6.7e-6	4.31e-7
12	0	0	1	3.33e-4	3.35e-4	1.61e-4	1.65e-4
13	0	0	2	2.6e-5	4.47e-6	7.9e-6	3.00e-6
14	0	0	3	3.8e-5	3.42e-6	8.7e-6	3.72e-7
15	0	1	1	1.43e-4	1.45e-4	6.7e-5	7.15e-5
16	0	1	2	2.1e-5	1.11e-6	7.1e-6	7.49e-7
17	0	1	3	2.2e-5	8.56e-7	7.1e-6	8.13-8
18	1	2	0	3.199e-3	3.1900e-3	2.106e-3	2.105e-3
19	1	3	0	9.84e-4	9.81e-4	6.46e-4	6.47e-4
20	1	4	0	3.11e-4	3.02e-4	2.00e-4	1.99e-4
21	1	2	2	2.0e-5	3.42e-7	6.8e-6	2.30e-7
22	1	3	2	1.6e-5	5.17e-7	6.6e-6	3.48e-7
23	1	4	2	1.8e-5	4.80e-7	6.7e-6	3.12e-7
24	2	3	0	3.92e-4	3.83e-4	2.54e-4	2.53e-4
25	2	2	2	2.0e-5	4.97e-7	7.4e-6	3.34e-7
26	2	3	2	1.5e-5	9.34e-7	6.8e-6	6.28e-7
27	2	4	2	1.7e-5	9.56e-7	6.7e-6	6.42e-7
28	0	2	2	3.0e-5	3.49e-7	7.8e-6	2.31e-7
29	control A only			4.4e-5	5.24e-5	1.8e-5	2.12e-5

4.1 Effect of Preview Length. "Optimal" feedforward controllers have been designed with $m = N = 0$ and different values of Np in order to study preview length effects (lines 1–11). The optimal costs obtained from the solution of (7) are here identical:

$$J_1^{\epsilon,\text{opt}} = J_\infty^{\epsilon,\text{opt}} = \begin{cases} 1, & N_p = 0 \\ |b|^{N_p - 1}, & N_p \geq 1 \end{cases} \tag{8}$$

Since $m = N = 0$, the model following error is equal to the actual tracking error, and it may be easily shown that tracking errors predicted using (8) fully agree with the theoretical errors obtained from simulation on lines 1–11. Good agreement between theoretical and experimental results is shown for $Np \leq 6$ although divergence due to unmodeled dynamics (including coulomb friction) occurs for larger Np values. While increasing Np theoretically continues to reduce tracking errors according to (8), experimental improvements were seen only up to $Np = 10$, with greater Np values providing no additional benefit.

For the reference trajectory utilized in this work, the addition of optimal feedforward control to the closed-loop feedback system actually increased both maximum and rms tracking errors for Np less than 8. This is explained by noting that the feedforward controllers are optimal over the entire class of bounded reference signals such that performance for any particular trajectory need not be improved. Indeed, the optimal feedforward controller for preview lengths of 0 or 1 turns out to be exactly the negative of the feedback controller, making the net control input to the plant zero. The plant response is thus zero for all time, giving a tracking error identically equal to the reference trajectory.

4.2 Effect of Tracking Constraint. The first significant point about the constrained optimal tracking problem is that a controller utilizing the presented $T(\lambda)$ constraint to only a few exponential degrees along with a single preview step can provide equal performance to a 9 or 10 preview step controller alone. This may be seen for example by comparing lines 11 and 16, where experimental maximum and rms results are nearly identical. Theoretical results, while not in as close agreement as their experimental counterparts, do show that the two controllers provide similar levels of performance.

Second, it is clear that increasing N theoretically improves tracking performance for the chosen trajectories. This trend may be followed in lines 12–17. Experimentally, however, this trend does not always hold and the reverse may in fact be true. For example, line 12 with $N = 1$ shows excellent agreement between experimental and theoretical results. Increasing N by one in line 13 shows dramatic performance improvements, although the experimental and theoretical results have begun to diverge. Now, line 14 shows the results of a further unit increase in N: theory shows an error decrease, while experimental errors have increased under both maximum and rms performance measures.

Finally, it might wrongly be expected that the $N = 3$ case of lines 14 and 17 would provide perfect theoretical tracking since the reference wave form is seemingly parabolic (i.e., comprised of step, ramp, and parabolic components). This is not the case however, since the trajectory is really a periodic signal and does not represent an infinitely long parabola. For perfect tracking, the constraint should be chosen as $T(\lambda) = (1 - \lambda^N)$, where N is the number of sampling periods in one trajectory cycle (e.g., 880 for the trajectory used here). Such a constraint choice would likely make the solution of the Bezout identity (6) exceedingly difficult and prone to numerical round-off sensitivity. In addition, the resulting controller would be of high order and computationally inefficient in that none of the transfer function coefficients will in general be zero. A feedback approach to repetitive control that results in less complicated controllers is presented in Alter and Tsao (1994).

4.3 Effect of Reference Model and Miscellaneous Observations. Reference model orders of $m = 0$, 1, and 2 were employed in this study, and at a sampling rate of 2000 Hz give a −3 dB reference model bandwidth of 364 Hz for $m = 1$, and 261 Hz for $m = 2$. The results show that in some cases, a unit increase in the reference model order produces theoretical and experimental performance improvements similar to those that would be obtained by a unit preview increase. This may be observed for example in lines 19, 20, and 24. In other cases, increasing m causes an increase in theoretical and experimental errors (compare, for example, the following line pairs: (21, 25), (22, 26), and (23, 27)). This is to be expected since increasing m decreases the ability of the reference model to itself track the high frequency trajectory components.

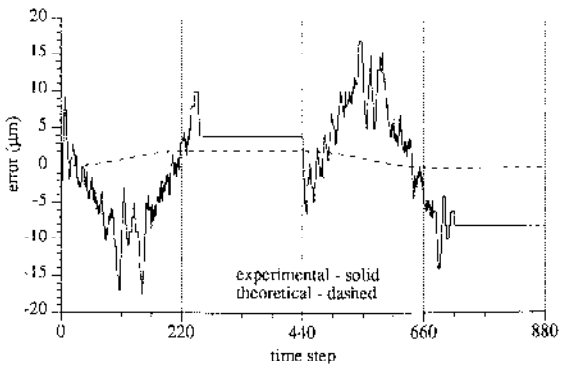

Fig. 3 Tracking error, $(m, N_p, N) = (0, 9, 0)$ with controller A

Table 2 Cost values for feedforward controllers

Design Parameters			$J_1 = \|M - GQ\|_1$		
m	N_p	N	$\lim_{\varepsilon \to 0} J_1^{\varepsilon}$	J_1^{opt}	$\|M\|_1$
0	9	0	1.60e-4	1.22e-4	2.94
0	1	2	1.171	0.895	5.657
2	3	2	0.0169	0.0129	2.205

As a general observation, the optimal controller design for line 28 is equivalent to the zero phase error tracking control (ZPETC) previously proposed in Tomizuka (1987). This generally nonoptimal controller happens to be optimal in the sense of $(m, Np, N) = (0, 2, 2)$ for a one unstable zero system such as the one here.

The actual tracking error time plot for a particular feedforward design is shown in Fig. 3. Noteworthy here is the significant experimental D.C. error which, as in the feedback only case, is being caused by coulomb friction. This D.C. error will be handled in the next section.

Finally, note that an analysis of plant unmodeled dynamics has explained well the mismatch between theoretical and experimental results in Table 1, although brevity precludes any discussion here. The reader is referred to Alter (1994) for a presentation of this as well as additional results.

5 Feedforward Designs With Integral Action Feedback

In this section, three optimal feedforward designs are presented for the linear motor servo loop using feedback controller B. The Corollary 1 requirement that $M(1) = 0$ is satisfied provided that $M_0(1) = 1$. The reference model should therefore be chosen with unity D.C. gain, which would typically be the case even for non-optimal tracking design. The zero-phase reference model being used in this research meets this requirement.

Preview and reference model degrees have been chosen so that the H_∞ and l_1 controllers obtained using the perturbation technique are the same. However, as the perturbation is reduced to zero, the feedforward controller does become H_∞ optimal, while remaining suboptimal for the l_1 norm. The l_1 suboptimality of the feedforward controllers has been summarized in Table 2. The last column of the table represents the l_1 norm with $Q = 0$ (i.e., no feedforward control action), giving a global perspective on the suboptimality of the perturbation design technique. From this viewpoint, the presented suboptimal l_1 controllers appear nearly optimal.

Table 3 Tracking results of optimal feedforward control designed for feedback controller B

#	Design Parameters			max. tracking error (m)		tracking error rms (m)	
	m	N_p	N	exper.	theor.	exper.	theor.
30	0	9	0	1.8e-5	8.14e-8	5.8e-6	3.98e-8
31	0	1	2	1.8e-5	1.11e-6	5.6e-6	7.49e-7
32	2	3	2	1.5e-5	9.34e-7	6.0e-6	6.28e-7
33	control B only			4.3e-5	2.76e-5	1.5e-5	1.58e-5

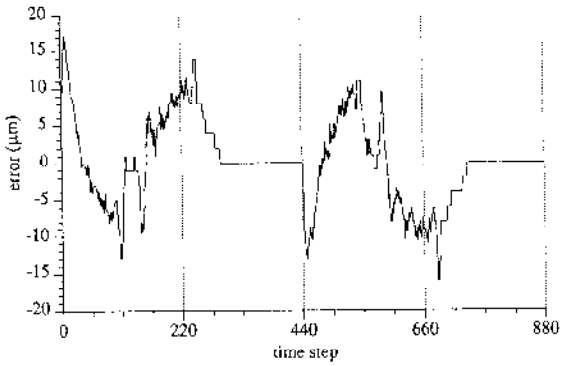

Fig. 4 Experimental tracking error, $(m, N_p, N) = (0, 9, 0)$ with controller B

Tracking error performance is given in Table 3, and may be compared with similar control A based designs in Table 1. Theoretical error values for the designs $(m, Np, N) = (0, 1, 2)$ and $(2, 3, 2)$ are seen identical between the controller A and B cases (up to the number of significant digits shown), although marked differences do occur in the $(0, 9, 0)$ design. Experimentally, the controller B designs show similar error values to the controller A designs. The motivation for using an integral-action feedback controller was the elimination of D.C. error, and the experimental error time response is shown in Figure 4 for one feedforward design. Clearly, the control B system has here achieved zero D.C. error. Experimental elimination of D.C. error has thus been achieved without a substantial increase in maximum or rms error.

6 Concluding Remarks

The implementation of optimal l_1 and H_∞ digital feedforward tracking control has been presented for a linear motor drive. The effects of preview length, tracking constraints, and the reference model have been illustrated in the experimental results. Prudent choice of these design parameters is important since it restricts the reference signals to a smaller class and results in tighter optimal tracking performance. For the practically important case of feedback controllers with integral action, a suboptimal l_1 solution has been derived and compared to the quantified optimal performance. Inevitable unmodeled dynamics make achieving arbitrarily small tracking errors impossible. Therefore, it makes no sense to design a feedforward tracking controller with arbitrarily higher bandwidth than the acceptable range of the unmodeled dynamics. An explicit relation between feedforward control bandwidth selection and the unmodeled dynamics is thus desirable and is of further research interest. For the specific trajectory employed here, the best performing feedforward controllers were experimentally seen to reduce by more than half the maximum and rms tracking errors of the optimal feedback loop.

The optimal feedforward control combined with the optimal feedback controllers given in (Alter and Tsao, 1996) represents a viable design approach for the control of linear motor feed drives for both high dynamic stiffness and optimal tracking performance.

References

Alter, D. M., and Tsao, T-C, 1995, "Control of Linear Motors for Machine Tool Feed Drives: H_∞ Optimal Feedback for Dynamic Stiffness," to appear ASME JOURNAL OF DYNAMIC SYSTEMS, MEASUREMENT, AND CONTROL.

Alter, D. M., 1994, *Control of Linear Motors for Machine Tool Feed Drives*, Ph.D. Dissertation, Univ. of Illinois at Urbana-Champaign.

Alter, D. M., and Tsao, T.-C., 1994, "2-D Exact Model Matching with Application to Repetitive Control," ASME JOURNAL OF DYNAMIC SYSTEMS, MEASUREMENT, AND CONTROL, Vol. 116, pp. 2–9.

Dahleh, M. A., and Pearson, J. B., 1987, "l^1-Optimal Feedback Controllers for MIMO Discrete-Time Systems," *IEEE Transactions on Automatic Control*, Vol. 32, No. 14, pp. 314–322.

Franklin, G. F., and Powell, J. D., 1981, *Digital Control of Dynamic Systems*, Addison-Wesley, Reading, MA, pp. 190–195.

Tomizuka, M., 1987, "Zero Phase Error Tracking Controller for Digital Control," ASME JOURNAL OF DYNAMIC SYSTEMS, MEASUREMENT, AND CONTROL, Vol. 109, pp. 65–68.

Tsao, T-C., 1994, "Optimal Feedforward Digital Tracking Controller Design," ASME JOURNAL OF DYNAMIC SYSTEMS, MEASUREMENT, AND CONTROL, Vol. 116, pp. 583–592.

Vidyasagar, M., 1991, "Further Results on the Optimal Rejection of Persistent Bounded Disturbances," *IEEE Transactions on Automatic Control*, Vol. 36, pp. 642–652.

Vidyasagar, M., 1985, *Control System Synthesis: A Factorization Approach*, The MIT Press, Cambridge, MA, pp. 174–178.

Zames, G., and Francis, B. A., 1983, "Minimax Sensitivity, and Optimal Robustness," *IEEE Transactions on Automatic Control*, Vol. 28, pp. 585–601.

Ziemer, R. E., Tranter, W. H., and Fannin, D. R., 1983, *Signals and Systems: Continuous and Discrete*, Macmillan, New York, pp. 388–419.

APPENDIX

Proof of Corollary 1

The proof for Corollary 1 involves the direct application of results previously published in Vidyasagar (1991). Although those results will not be reviewed here, similar notation has been adopted where possible to simplify referencing. We first find the optimal cost value by applying Theorem 3.6 of that work. We have the unit circle zero of $G(\lambda)$ defined by $\lambda_1 = 1$, and the unstable zero of $G(\lambda)$ defined by $z_1 = b$. From the corollary statement we note that $M(\lambda_1) = M(1) = 0$. Therefore:

$$J_1^{\text{opt}} = \max_{a_1, a_{1,0}} |a_1 M(\lambda_1) + b_{1,0} M(z_1)| - \max_{b_{1,0}} |b_{1,0} M(b)|$$

subject to the constraint

$$\| a_1 \phi_i - b_{1,0} \theta_{i,0} \|_\infty \leq 1$$

where a_1 and $b_{1,0}$ are real numbers, and the sequences ϕ_i and θ_i are given by

$$\phi_i = \{\lambda_1^s\}_{s=0}^{\infty} = \{1, 1, 1, \ldots\}$$

$$\theta_{i,0} = \{z_1^s\}_{s=0}^{\infty} = \{1, b, b^2, \ldots\}.$$

The constraint thus simplifies to: $|a_1 + b_{1,0} b^i| \leq 1$, $i = 0, 1, 2, \ldots$. Since $b < 0$, and $|b| < 1$, constraints other than for $i = 0$, $i = 1$, and $i \to \infty$ are redundant. The region satisfying the active constraints is graphically shown in Fig. A.1. The maximizing choice of $b_{1,0}$ is determined from the intersections of the $i = 0$ and $i = 1$ constraints:

$$b_{1,0} = \frac{2}{1 - b} \operatorname{sgn} \{M(b)\}$$

where sgn denotes the sign function. Hence $J_1^{\text{opt}} = (2/(1 - b))|M(b)|$.

We next utilize Dahleh and Pearson (1987) to solve the related optimization problem where G has been replaced with G_∞, resulting in

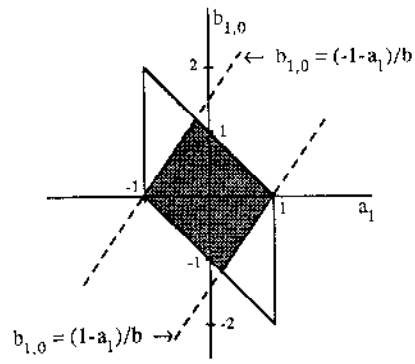

Fig. A-1 Geometric region satisfying constraints

$$Q_0 := G_o^{-1}\frac{(1-b\lambda)}{(\lambda-b)}[M(\lambda)-M(b)]$$

$$\text{and} \quad \Phi_0 := M - G_o Q_0 = M(b).$$

Finally, lemma 4.3 from Vidyasagar's work is applied to compute the limit of J_3:

$$\lim_{\epsilon\to 0}\|M - GQ_\epsilon\|_1 = \|\Phi_0\|_1 + |\Phi_0(1)| = |M(b)| + |M(b)|$$

$$= 2|M(b)|.$$

□

Contact/Impact in Hybrid Parameter Multiple Body Mechanical Systems—Extensions for Higher-Order Continuum Models

Alan A. Barhorst[1]

In recent work the author presented a systematic formulation of hybrid parameter multiple body mechanical systems (HPMBS) undergoing contact/impact motion. The method rigorously models all motion regimes of hybrid multiple body systems (i.e., free motion, contact/impact motion, and constrained motion), utilizing minimal sets of hybrid differential equations; Lagrange multipliers are not required. The contact/impact regime was modeled via the idea of instantaneously applied nonholonomic constraints. The technique previously presented did not include the possibility of continuum assumptions along the lines of Timoshenko beams, higher order plate theories, or rational theories considering intrinsic spin-inertia. In this technical brief, the above-mentioned method is extended to include the higher-order continuum assumptions which eliminates the continuum shortfalls from the previous work. The main contributions of this work include: 1) the previous work is rigorously extended, and 2) the fact that coefficients of restitution are not required for modeling the momentum exchange between motion regimes of HPMBS. The field and boundary equations provide the needed extra equations that are used to supply post-collision pointwise relationships for the generalized velocities and velocity fields.

Introduction

There is a considerable amount of work on contact and impact being recently reported in the literature. Researchers are examining the viability of coefficients of restitution in rigid body collisions; examining friction during contact and impact; examining three-dimensional rigid-body collisions with friction; and examining general contact problems (Nasser, 1992; Stronge, 1994; Kishore et al., 1994; Park and Kwak, 1994; Laursen and Oancea, 1994; Yen and Wu, 1995; Marghitu and Hurmuzlu, 1995; Bhatt and Koechling, 1995a; Wang et al., 1995; Bhatt and Koechling, 1995b; Batlle, 1996; Villaggio, 1996; Stoianovici and Hurmuzlu, 1996).

In this technical brief, the modeling methodology described in Barhorst and Everett, (1995b) and Barhorst (1997b) will be used to extend the hybrid parameter multiple body mechanical systems (HPMBS) contact/impact model presented in Barhorst and Everett (1995a). The extension to the previous work is required because it lacks consideration for intrinsic inertia properties of continuum bodies in the multiple body system. The adjustments needed are straightforward to implement, but this simplicity obscures the true advantage of the extension; namely, it provides other impulse-momentum equations for determining the after contact/impact velocity field. These extra equations delete the shortcomings of the modeling method presented in Barhorst and Everett (1995a).

One of the advantages of using the approach described earlier and completed herein is that rarely are coefficients of restitution needed to describe the collision, because, in this technique the field equations of motion supply the needed extra equations of impact.

Derivation

In this section a résumé of the formulas that extend the previously mentioned less general method are provided. The details of the derivation are not significantly different from the derivation details of the previous less general set of equations, and thus are not provided. However, the intermixed discussion should allow the interested reader to generate the equations.

Ordinary Impulse—Momentum Equations

The ordinary differential equations (ODE) of motion that model the overall motion of a HPMBS can be written as shown previously (Barhorst and Everett, 1995b; Barhorst and Everett, 1995a; Barhorst, 1997b).[2] By examining the time integral of the ODE as time shrinks to the time of contact/impact results in the following generalized momentum equations. The evaluation of the partial velocities at the time just before impact t_o^- is justified via Taylor series expansion of the partial velocity terms.[3] The equations are:

$$0 = \sum_r \left\{ \left.\frac{\partial {}^o_N\vec{v}^{s_r}}{\partial s_n}\right|_{t_o^-} \cdot [\vec{F}_r - (\dot{\vec{L}}_r(t_o^+) - \dot{\vec{L}}_r(t_o^-))] \right.$$

$$\left. + \left.\frac{\partial {}^N\vec{\omega}^{B_r}}{\partial s_n}\right|_{t_o^-} \cdot [\vec{T}_r - (\dot{\vec{H}}_r(t_o^-) - \dot{\vec{H}}_r(t_o^-))] \right\}$$

$$- \sum_r \left\{ \left.\frac{\partial {}^o_N\vec{v}^{s_r}}{\partial s_n}\right|_{t_o^-} \cdot [\vec{F}_r - (\dot{\vec{L}}_r(t_o^+) - \dot{\vec{L}}_r(t_o^-))] \right.$$

$$\left. + \left.\frac{\partial {}^N\vec{\omega}^{B_r}}{\partial s_n}\right|_{t_o^-} \cdot [\vec{T}_r - (\dot{\vec{H}}_r(t_o^+) - \dot{\vec{H}}_r(t_o^-))] \right\} \quad (1)$$

The individual terms are defined as follows:

$\vec{F}_r$ = Resultant active impulse of force on body r.

$\vec{L}_r = m^o_{rN}\vec{v}^{*_r}$, linear momentum of body r.

$\vec{T}_r$ = Moment of all non-constraint impulses of forces about the point s_r including impulses of couples.

$$\vec{H}_r = {}^{s_r}\vec{r}^{*_r} \times m^o_{rN}\vec{v}^{s_r} + \bar{\bar{I}}_{s_r} \cdot {}^N\vec{\omega}^{B_r}$$

[1] Assistant Professor, Mechanical Engineering, Texas Tech University, Lubbock, Texas 79409-1021. Mem. ASME.

Contributed by the Dynamic Systems and Control Division of THE AMERICAN SOCIETY OF MECHANICAL ENGINEERS. Manuscript received by the Dynamic Systems and Control Division November 12, 1996. Associate Technical Editor: R. Redfield.

[2] The Nomenclature also follows the previous work.

[3] See the discussion relative to instantly applied nonholonomic constraints in the section title "Comments."